

to the most probable values of  $P$ . The disagreements at 16 MeV thus do not appear to be as statistically significant as the agreement at 24 MeV. There appears to be here, therefore, a partial, though still rather inaccurate, confirmation of charge independence of nuclear forces as applied essentially to the spin-orbit part of the nucleon-nucleon interaction. The situation is illustrated in Fig. 6. If experiments of higher accuracy could be performed, more accurate information regarding the applicability of charge independence to this component of the nucleon-nucleon interaction would be obtained.

It should be remarked that plots of  $P$  against angle at 37 and 52.5 MeV show a marked trend for  $P(45^\circ)$  to

be low as compared with theoretical expectation. This lack of internal consistency in the comparison of theory and experiment is an additional reason for regarding the attempt at the test of charge independence for spin-orbit component of the interaction as preliminary.

#### ACKNOWLEDGMENTS

The writers are indebted to Dr. Taylor and Dr. Christmas for communicating to them their data before publication and for permission to refer to them, to Miss J. Gibson for expert mathematical assistance, and to F. A. McDonald and R. G. Brandt for their help at various stages of the work.

### Phase-Parameter Representation of Neutron-Proton Scattering from 13.7 to 350 MeV. II\*

M. H. HULL, JR., K. E. LASSILA, H. M. RUPPEL, F. A. McDONALD, AND G. BREIT  
Yale University, New Haven, Connecticut

(Received June 11, 1962)

Phase parameters for fits YLAN3M and YLAN1 to  $n$ - $p$  scattering data are presented in the form of graphs suitable for quantitative application. (Additional tabulated material is available from the American Documentation Institute.) Modifications in YLAN3M arising from the use of a potential are recorded with special attention to lower energies.

#### I. INTRODUCTION

SINCE the publication of phase-parameter representations of neutron-proton scattering by the Yale group,<sup>1</sup> a number of requests for more detailed numerical information have been and continue to be received. In order to satisfy these demands more efficiently, graphs and tables of the phase parameters for some of the fits have been prepared and are in part reproduced below. Supplementary material is also being made available.<sup>2</sup>

The notation used is essentially the same as in reference 1. Triplet phase shifts for orbital angular momentum  $L\hbar$  and total angular momentum  $J\hbar$  are denoted by  ${}^3\delta_{LJ}$ ; for coupled states, the matrix  $U$  is parametrized in terms of the quantities  ${}^3\theta_{LJ}$  and  $\rho_J$ ; for the superscripts, the spectroscopic equivalent of  $L$ , such

as  $P$  for  $L=1$ , is often used; singlet phase shifts for angular momentum  $J\hbar$  are designated by  $K_J$ .

#### II. GRAPHICAL REPRESENTATION OF YLAN1 AND YLAN3M

Figures 1, 2, 3, 4 and 5 show the phase parameters for the results of searches YLAN1 and YLAN3M of reference 1, the latter appearing as the more likely among the six previously presented. From a purely statistical viewpoint of the value of the mean-square deviation YLAN1 is among the poorer fits, but the purely statistical criterion may not be very reliable in this case. While it belongs in the same class with YLAN3M and YLAN3 regarding the classification of fits according to values of  $\rho_3$  and  $K_3$ , the sign for  $\rho_1$  for it is like that of YLAN3M rather than of YLAN3 and is more likely to be the right one if one may judge from predictions of potential models.

In Fig. 1 are shown  $K_1$  and  $K_3$ . Figure 2 contains plots of  ${}^3\theta_{S_1}$  and  ${}^3\theta_{D_1}$ . Figure 3 displays  ${}^3\theta_{D_2}$  and  ${}^3\theta_{D_3}$ . Figure 4 gives a graphical representation of the coupling parameters  $\rho_1$ ,  $\rho_3$  and  $\rho_5$ , while Fig. 5 represents  ${}^3\theta_{G_3}$ ,  ${}^3\theta_{G_4}$ , and  ${}^3\theta_{G_5}$ . In all cases, angles are in radians and the incident energy in the laboratory system is in MeV. Phase parameters not shown in the graphs have been given their OPEP (one-pion exchange potential) values.

\* This research was supported by the U. S. Atomic Energy Commission and by the U. S. Army Research Office (Durham).

<sup>1</sup> M. H. Hull, Jr., K. E. Lassila, H. M. Ruppel, F. A. McDonald, and G. Breit, *Phys. Rev.* **122**, 1606 (1961).

<sup>2</sup> This material has been deposited as Document No. 7282 with the ADI Auxiliary Publications Project, Photoduplication Service, Library of Congress, Washington 25, D. C. A copy may be secured by citing the Document number and by remitting \$2.50 for photoprints, or \$1.75 for 35 mm microfilm. Advance payment is required. Checks or money orders are to be made payable to: Chief, Photoduplication Service, Library of Congress.

<sup>3</sup> K. E. Lassila, M. H. Hull, Jr., H. M. Ruppel, F. A. McDonald, and G. Breit, *Phys. Rev.* **126**, 881 (1962).

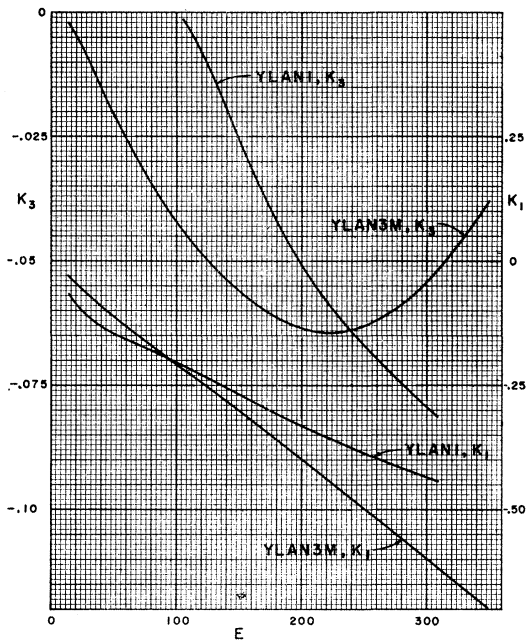


FIG. 1. Phase shifts  $K_1$ ,  $K_3$  in radians plotted against incident laboratory energy in MeV.

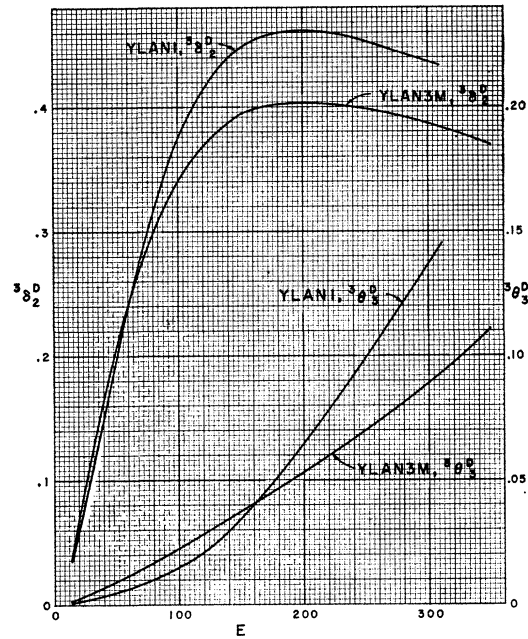


FIG. 3. Phase parameters  $3\theta_2^D$  and  $3\theta_3^D$  in radians plotted against incident laboratory energy in MeV.

Arrangements referred to previously<sup>2</sup> make available tables of values of phase parameters for fits YLAN3M, YLAN3, YLAN2M, and YLAN2 at 20 experimental energies covering the range from 13.7 to 310 MeV. It should be emphasized that the work reported on in reference 1 was primarily intended to provide an over-all

representation of the data above 13.7 MeV and that the joining of the data to lower energies was not as smooth as would be justifiable by the accuracy of information concerning scattering lengths and the deuteron binding energy. This defect has been largely removed in the

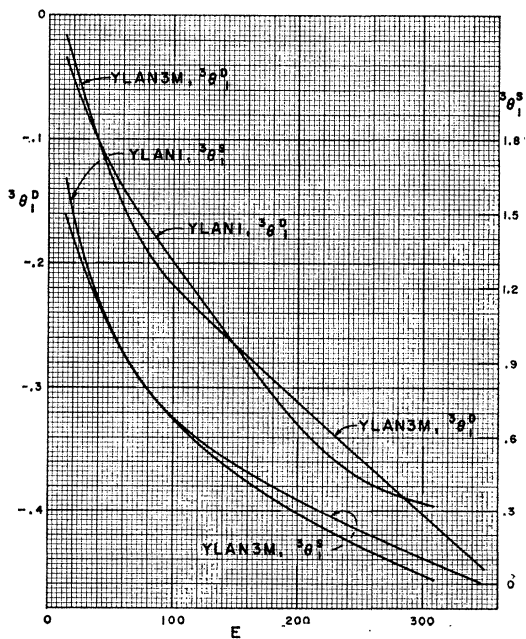


FIG. 2. Phase parameters  $3\theta_1^S$  and  $3\theta_1^D$  in radians plotted against incident laboratory energy in MeV.

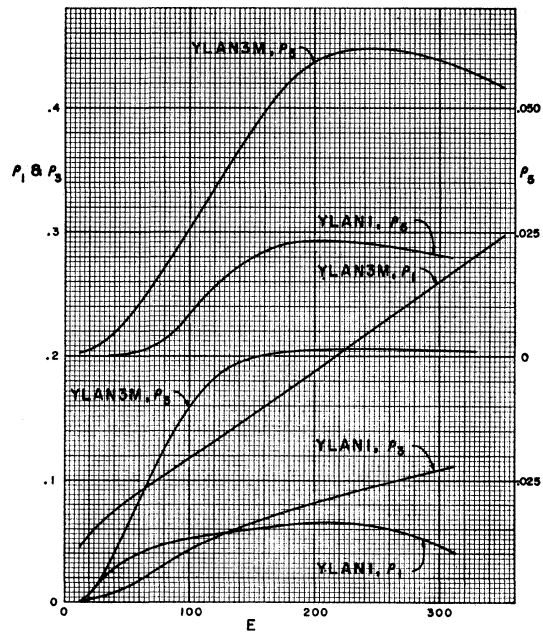


FIG. 4. Phase parameters  $\rho_1$ ,  $\rho_3$ ,  $\rho_5$  plotted against incident laboratory energy in MeV. The sign of  $\rho_1$  in these graphs is consistent with predictions of  $n$ - $p$  potentials adjusted to the deuteron ground state properties.

TABLE I. Phase parameters for  $T=0$  states calculated from a potential adjusted to the deuteron ground state and fit YLAN3M. Values are in radians.

$E$ (MeV)	$K_1$	$K_3$	${}^3\theta_1^S$	$\rho_1$	${}^3\theta_1^D$	${}^3\theta_2^D$	${}^3\theta_3^D$	$\rho_3$	${}^3\theta_3^G$	${}^3\theta_4^G$	${}^3\theta_5^G$	$\rho_5$
5	-0.0226	-0.0002	2.0653	0.0228	-0.0031							
10	-0.0449	-0.0011	1.7957	0.0429	-0.0115							
15	-0.0623	-0.0027	1.6305	0.0530	-0.0222							
25	-0.0879	-0.0069	1.4171	0.0688	-0.0464	0.0652	0.0026	0.0195	-0.0008	0.0031	-0.0002	0.0016
50	-0.1323	-0.0172	1.1129	0.0915	-0.1055	0.1539	0.0094	0.0555	-0.0043	0.0130	-0.0006	0.0075
100	-0.2149	-0.0288	0.7826	0.1333	-0.2017	0.2858	0.0269	0.1182	-0.0146	0.0390	-0.0014	0.0255
150	-0.3032	-0.0329	0.5717	0.1757	-0.2766	0.3598	0.0428	0.1634	-0.0264	0.0644	-0.0017	0.0443
200	-0.3921	-0.0349	0.4119	0.2184	-0.3382	0.3955	0.0550	0.1971	-0.0380	0.0865	-0.0015	0.0615
250	-0.4786	-0.0372	0.2811	0.2613	-0.3908	0.4072	0.0633	0.2239	-0.0489	0.1047	-0.0010	0.0767
300	-0.5617	-0.0409	0.1694	0.3032	-0.4367	0.4036	0.0683	0.2463	-0.0590	0.1192	-0.0006	0.0903
330	-0.6098	-0.0439	0.1090	0.3279	-0.4617	0.3965	0.0700	0.2582	-0.0647	0.1261	-0.0004	0.0976

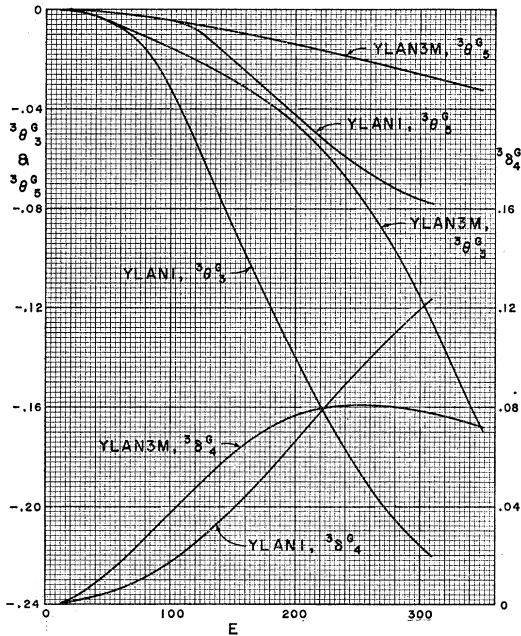
work of Lassila, Hull, Ruppel, McDonald, and Breit<sup>3</sup> in which a potential is made to fit the data below 13.7 MeV and YLAN3M above this energy. The low-energy information includes values of the binding energy of the deuteron and the triplet scattering lengths and effective range. The electric quadrupole moment of the deuteron was not directly used in the adjustment but the value calculated from the potential is only about 0.75% below the experimental. A few values obtained by means of this potential, showing characteristic differences from YLAN3M, are shown in Table I.

The published Yale potential for  $T=1$  has been obtained employing YLAM values supplemented by low-energy  $p$ - $p$  data. Adjustment to reproduce the experi-

mental  $n$ - $p$  scattering length requires an increase of the  ${}^1S_0$  potential well depth by about 1.69%. The changed depth gives an absolute value of the singlet  $n$ - $p$  scattering length of  $23.69 \times 10^{-13}$  cm which agrees with the value  $(23.68 \pm 0.06) \times 10^{-13}$  cm listed by Salpeter<sup>4</sup> and the newer value  $(23.67 \pm 0.06) \times 10^{-13}$  cm of Passell.<sup>5</sup>

TABLE II. Phase shift in  ${}^1S_0$  state calculated from a potential adjusted to the fit to  $p$ - $p$  data and one obtained by increasing the  $p$ - $p$  depth by 1.69% to allow a fit to the singlet scattering length from low energy  $n$ - $p$  scattering. For direct comparison with the  $p$ - $p$  nuclear force potential, its Coulomb part was omitted in calculating  $(K_0')_{p-p}$ .

$E$ (MeV)	$(K_0)_{n-p}$	$(K_0')_{p-p}$
2	1.1162	1.0271
4	1.1077	1.0406
5	1.0952	1.0340
6	1.0812	1.0244
8	1.0524	1.0021
10	1.0243	0.9784
15	0.9598	0.9209
25	0.8524	0.8206
50	0.6553	0.6309
100	0.3912	0.3721
150	0.2009	0.1842
200	0.0475	0.0323
250	-0.0831	-0.0973
300	-0.1981	-0.2115
330	-0.2614	-0.2745

FIG. 5. Phase parameters  ${}^3\theta_3^G$ ,  ${}^3\theta_4^G$ ,  ${}^3\theta_5^G$  in radians plotted against incident laboratory energy in MeV.

The  $n$ - $p$  singlet effective range corresponding to this potential is  $2.80 \times 10^{-13}$  cm in fair agreement with values listed by Salpeter.<sup>4</sup> The difference in  $K_0$  caused by the 1.69% increase in potential well depth is illustrated in Table II. The  $(K_0')_{p-p}$  in the table is the value of  $(K_0)_{p-p}$  with the  $e^2/r$  removed from the total potential energy.

#### ACKNOWLEDGMENT

Miss J. Gibson's expert mathematical assistance is gratefully acknowledged.

<sup>4</sup> E. E. Salpeter, Phys. Rev. 82, 60 (1951).

<sup>5</sup> L. Passell (private communication).